

Solar system peculiar motion from the Hubble diagram of quasars and testing the Cosmological Principle

Ashok K. Singal^{*}

Astronomy and Astrophysics Division, Physical Research Laboratory, Navrangpura, Ahmedabad - 380009, India

Accepted XXX. Received YYY; in original form ZZZ

ABSTRACT

We determine here peculiar motion of the Solar system, first time from the $m - z$ Hubble diagram of quasars. Observer's peculiar motion causes a systematic shift in the $m - z$ plane between sources lying along the velocity vector and those in the opposite direction, providing a measure of the peculiar velocity. Accordingly, from a sample of $\sim 1.2 \times 10^5$ mid-infrared quasars with measured spectroscopic redshifts, we arrive at a peculiar velocity ~ 22 times larger than that from the CMBR dipole, but direction matching within $\sim 2\sigma$. Previous findings from number count, sky brightness or redshift dipoles observed in samples of distant AGNs or SNe Ia too had yielded values two to ten times larger than the CMBR value, though the direction in all cases agreed with the CMBR dipole. Since a genuine solar peculiar velocity cannot vary from one dataset to the other, an order of magnitude, statistically significant, discordant dipoles, might imply that we may instead have to look for some other cause for the genesis of these dipole, including that of the CMBR. At the same time, a common direction for all these dipoles, determined from completely independent surveys by different groups employing different techniques, might indicate that these dipoles are not resulting from some systematics in the observations or in the data analysis, but could instead suggest a preferred direction in the Universe due to an inherent anisotropy, which, in turn, would be against the Cosmological Principle (CP), the most basic tenet of the modern cosmology.

Key words: quasars: general – cosmic background radiation – cosmological parameters – large-scale structure of Universe – cosmology: miscellaneous

1 INTRODUCTION

According to the CP, the universe should appear isotropic, without any preferred directions, to a comoving observer, having no peculiar motion relative to the cosmic fluid of the expanding universe. To such an observer the average properties of a given class of distant astronomical objects in the universe should appear statistically to have similar distributions in various directions. However a peculiar motion of such an observer might introduce a dipole anisotropy in the observed properties of a class of objects and which, in turn, might be exploited to infer the peculiar velocity of the observer. For instance, the Cosmic Microwave Background Radiation (CMBR) shows an isotropic distribution except for a dipole anisotropy which, when ascribed to a peculiar motion of the observer, has given a peculiar velocity of the solar system to be 370 km s^{-1} along $\text{RA} = 168^\circ$, $\text{Dec} = -7^\circ$ in the sky (Lineweaver et al. 1996; Hinshaw et al. 2009; Aghanim et al. 2018).

Another such quantity that could be employed to look for departures from isotropy of the universe is the angular distribution of distant radio sources in the sky. This could provide an independent check on the interpretation of CMBR

dipole anisotropy being due to the observer's motion since an effect of the observer's motion should show up as a dipole anisotropy in sky distribution of the radio source population too. Also, while CMBR provides information about the isotropy of the universe for redshift $z \sim 1100$, the radio source population refers to a much later epoch $z \sim 1 - 3$. Thus it also provides an independent check on the CP for the matter universe, as isotropy of the Universe is assumed for matter and radiation *for all epochs*. In last one decade, peculiar motions determined from the number counts, sky brightness or redshift distributions in large samples of distant active galactic nuclei (AGNs) have yielded peculiar velocities two to ten times larger than that from the CMBR, although in the same direction as the CMBR dipole (Singal 2011; Rubart & Schwarz 2013; Tiwari et al. 2015; Colin et al. 2017; Bengaly, Maartens & Santos 2018; Singal 2019a,b; Secrest et al. 2021; Singal 2021a,b). A more recent determination of the peculiar velocity of the Solar system from a sample of supernovae type Ia (SNe Ia), has yielded a value about 4 times the CMBR value, again along the same direction (Singal 2021c).

These findings of the AGN and SNe Ia dipoles being much larger than the CMBR value (Singal 2011; Rubart & Schwarz 2013; Tiwari et al. 2015; Colin et al. 2017; Bengaly, Maartens & Santos 2018; Singal 2019a,b; Secrest et al. 2021; Singal 2021a,b,c) cast doubts on the CMBR dipole as being the

^{*} E-mail: ashokkumar.singal@gmail.com

ultimate representatives of the solar peculiar motion. While the CMBR dipole refers to the radiation era ($z \sim 1100$), AGN and SNe Ia dipoles represent the much later matter era ($z \sim 1-3$). The matching of their directions also shows that different dipoles are not because of some totally independent, random origins, nor could we say that the CMBR dipole is the one which is to be considered as more fundamental than the other ones for establishing the CP. Because of the impact of any genuine variation in the peculiar motion, determined from different samples or techniques, could be of such wide ramifications, it is important to be able to get peculiar motion from independent data, and possibly using independent technique.

Here, we determine peculiar motion of the Solar system, first time from the magnitude-redshift ($m-z$) Hubble diagram of quasars. Owing to the Doppler effect, arising from the peculiar motion of the observer, the observed intensity and redshift of a distant quasar get modified, giving rise to a small but finite displacement of a source in the $m-z$ plane. The extent and direction of the displacement in the $m-z$ plane is determined by the projection of the observer's peculiar motion along the sky position of the quasar. The quasars lying in the hemisphere centred on the pole of the peculiar motion undergo in the $m-z$ plot displacements opposite to those of the quasars lying in the opposite hemisphere, centred on the anti-pole. As a result, in the Hubble diagram, there occurs a systematic shift between sources lying in the hemisphere along the peculiar motion and those lying in the opposite hemisphere and this shift could provide a measure of the peculiar velocity of the observer. Such a technique was applied recently (Singal 2021c) to a sample of supernovae type Ia (SNe Ia), to determine the peculiar velocity of the Solar system from the magnitude-redshift Hubble diagram for the SNe Ia, one of the best standard candles known. Here we extend this technique to determine the peculiar velocity of the Solar system, first time from the magnitude-redshift Hubble diagram of quasars. As is well known, unlike SNe Ia, there is a large spread in the Hubble diagram of quasars, we would require a much larger sample to get any meaningful values for the peculiar motion. Moreover it would be helpful if the sample of quasars has the magnitude determination from a single instrument to minimize the spread in magnitude values from errors due to differential calibrations and any systematic differences in different instruments at different colors. Accordingly, we determine our peculiar motion from a large sample of $\sim 1.2 \times 10^5$ quasars, with mid-infrared magnitudes and measured spectroscopic redshifts.

2 PECULIAR MOTION FROM THE HUBBLE DIAGRAM OF QUASARS

According to the CP, an observer comoving with the cosmic fluid would find observed relations between any properties of distant objects, e.g., the redshift-magnitude Hubble diagram of quasars, apart from any statistical scatter, to be independent of direction. On the contrary, an observer moving with a peculiar velocity, might find a dipole anisotropy in some of the observed properties. By observing such variation over sky for a sufficiently large sample of sources, one could compute the peculiar velocity of the observer with respect to the comoving coordinates.

Peculiar velocity of the observer gives rise to the Doppler effect, modifying the observed redshift and optical magnitude of an object. Assuming the peculiar velocity v of the observer to be non-relativistic ($v \ll c$), as indicated by all previous measurements (Aghanim et al. 2018; Singal 2011, 19a,b; Secrest et al. 2021; Singal 2021b,c) c being the speed of light in vacuum. For a source lying at an angle θ with respect to the direction (pole) of the peculiar motion, as seen by the observer, the Doppler factor $[\gamma(1 - (v/c)\cos\theta)]^{-1}$, with $\gamma = \sqrt{1 - (v/c)^2}$ being the Lorentz factor, reduces for $v \ll c$ to $[(1 - (v/c)\cos\theta)]^{-1}$. Then the observed flux density of the source would be affected by

$$S = S_o(1 - (v/c)\cos\theta)^{-2}, \quad (1)$$

where S_o is the flux density as measured by a comoving observer, i.e., for a nil peculiar motion of the observer. Here one factor of $(1 - (v/c)\cos\theta)$ arises because of the shift in the frequency of each photon, while another similar factor arises from the change in number of photons arriving per unit time at the observer. It should be noted that one expects the ratio between the number densities as well as the sky intensities for the observer with a peculiar motion and the one stationary with respect to the comoving coordinates to have another factor of $(1 - (v/c)\cos\theta)^{-2}$ because of aberration, due to which the observed differential solid angle will be narrower by a factor

$$d\Omega = d\Omega_o(1 - (v/c)\cos\theta)^2. \quad (2)$$

where $d\Omega_o$ is the solid angle for the stationary observer. Therefore, an observer with a peculiar motion, in comparison to a comoving observer at the same location in the cosmic fluid, would observe higher number densities as well as sky intensities. However, the observed flux density of individual sources will remain unaffected by this extra factor.

Then the observed redshift and optical magnitude of an individual source are given by (Davies et al. 2011)

$$(1+z) = (1+z_o)(1 - v\cos\theta/c), \quad (3)$$

$$m = m_o + 5\log(1 - v\cos\theta/c), \quad (4)$$

where m_o and z_o are the values as would be measured by the comoving observer, without a peculiar motion. From the CP, m_o and z_o should have isotropic distributions.

For a given v of the observer, different sources, depending upon their θ , will get displaced in the $m-z$ plot differently. As the effects on both m and z are proportional to $\cos\theta$, all source with $\cos\theta > 0$, and thus lying in a hemisphere, say Σ_1 , centred on the pole, will get displaced in the $m-z$ plot opposite to the sources with $\cos\theta < 0$ and thus lying in the opposite hemisphere, say Σ_2 centred on the anti-pole. Accordingly, there will be a systematic displacement between sources belonging to Σ_1 and Σ_2 , and we could utilize this shift to get a handle on the peculiar velocity of the observer.

3 OUR SAMPLE OF QUASARS

Our sample of quasars is selected from a larger all-sky sample of 1.4 million active galactic nuclei (AGNs), which is publicly available (Secrest et al. 2015), and is derived in turn from the Wide-field Infrared Survey Explorer final catalog release (All-WISE), incorporating data from the WISE Full Cryogenic, 3-Band Cryo and NEOWISE Post-Cryo survey (Wright et al.

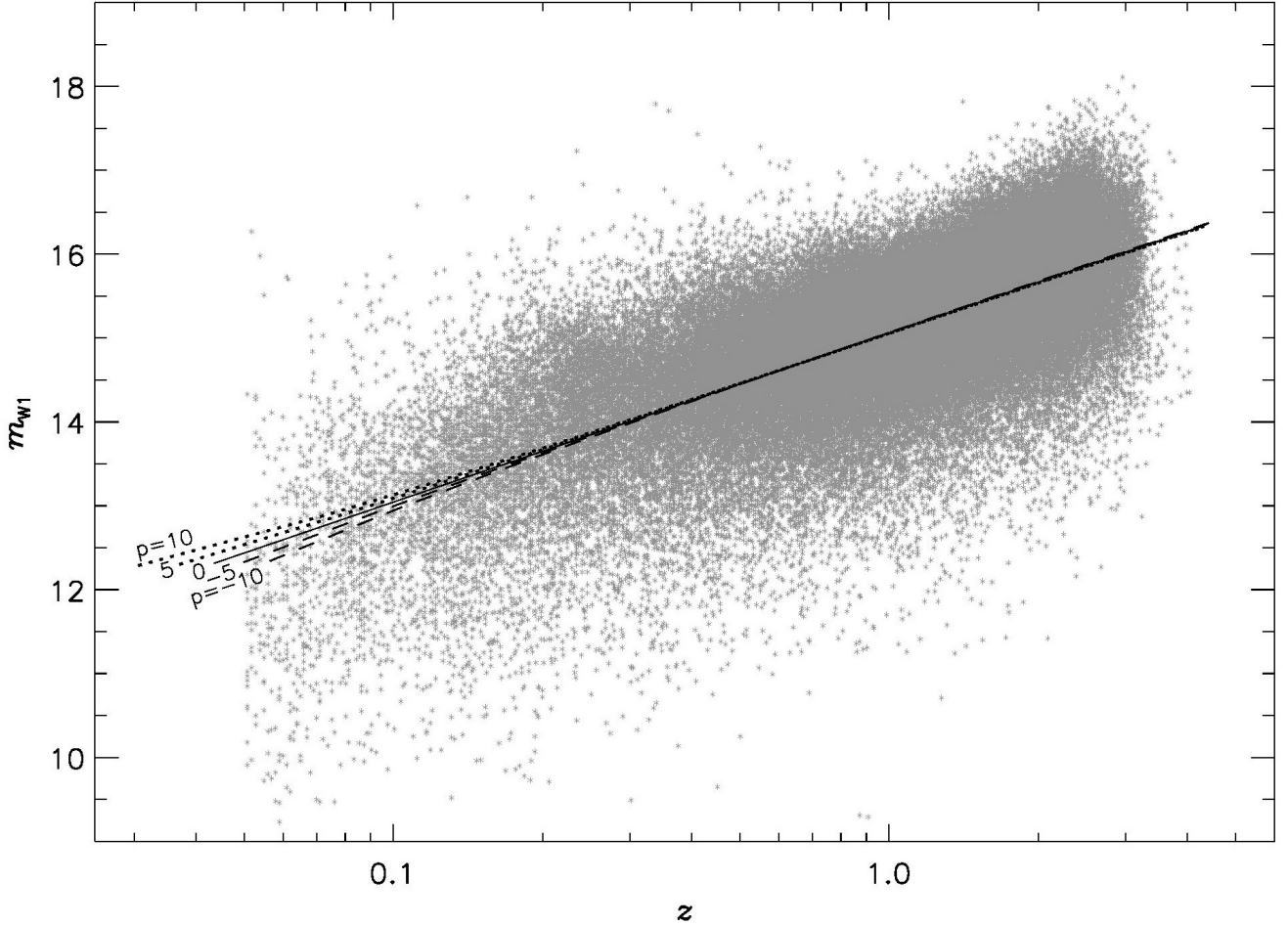


Figure 1. The observed Magnitude-redshift Hubble ($m_{w1} - z$) diagram for our sample of quasars with known spectroscopic redshifts. The continuous line in the middle shows the best fit ($m_{w1} \propto \log z$) to all quasars in our sample. Due to observer’s peculiar velocity, assumedly along the CMBR dipole, individual sources at any point in the $m_{w1} - z$ diagram would get displaced, with the displacement being, to a first order, directly proportional to the amplitude of the peculiar velocity, assumed to be a small non-relativistic value. To get an idea of the loci of the expected displacements, the dotted lines above the continuous line (i.e., at higher m_{w1}) show the displacements expected for different amplitudes of the peculiar velocity (quantified by p , in units of the CMBR value of 370 km s^{-1}), for sources lying in the direction (pole) of the peculiar velocity at its apex, while the dashed lines below the continuous line show loci of the displacements expected for sources lying in the anti-pole direction, for different p values ($p < 0$ in the anti-pole direction). It is clear that the displacements become appreciable only at low redshifts ($z \lesssim 0.5$).

2010; Mainzer et al. 2014). The WISE survey is an all-sky mid-infrared survey at 3.4 , 4.6 , 12 and $22 \mu\text{m}$ ($w1$, $w2$, $w3$ and $w4$) with angular resolutions 6.1 , 6.4 , 6.5 and 12 arc-sec, respectively. We have selected all quasars with measured spectroscopic redshifts from the original sample (Secrest et al. 2015) of ~ 1.4 million objects that met a two-color infrared photometric selection criteria for AGNs, out of the AllWISE catalog of almost 748 million objects.

The sample of known-spectroscopic redshift quasars, spans a redshift range 0.01 - 7.01 . However, we have restricted for our purpose the lower limit to 0.05 in order to keep the effect of local bulk flows to a minimum. Further, there is a sharp drop in number of quasars beyond $z > 4$, which we have excluded leaving us with a total of 115610 quasars in our sample, all outside the galactic plane ($b > 10^\circ$). The infrared magnitude

$w1$ provides a uniform measure at a single magnitude band for all quasars in our sample.

Figure 1 shows a $m_{w1} - z$ plot for all 115610 quasars in our sample, along with a best fit of a straight line ($m_{w1} \propto \log z$) to the data. It should be noted that the figure displays the m_{w1} range 9.0 - 19.0 , there are a small number of quasars outside this range, which are not shown in the figure to avoid getting the displayed magnitude scale compressed too much, but otherwise all these quasars are used in our computations. In Fig. 1, the continuous line in the middle shows the best fit ($m_{w1} \propto \log z$) to all quasars in our sample. Due to a peculiar motion of the observer, there could be alterations in the $m_B - z$ plot.

Due to observer’s peculiar velocity, assumedly along the CMBR dipole, individual sources at any point in the $m_{w1} - z$ diagram would get displaced, with the displacement being,

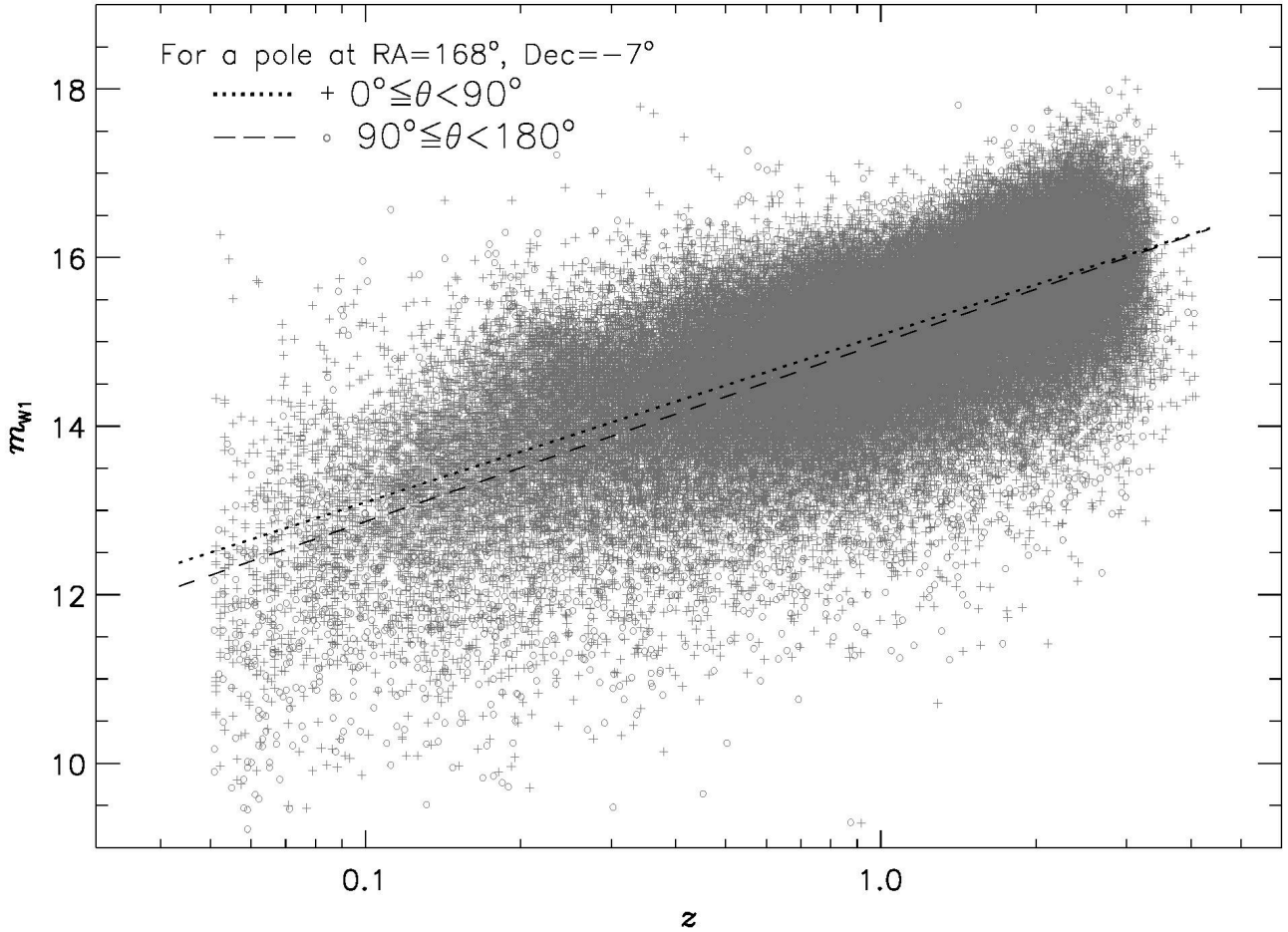


Figure 2. The observed Magnitude-redshift Hubble ($m_{w1} - z$) diagram for our sample of quasars with known spectroscopic redshifts. The dotted line shows the straight line ($m_{w1} \propto \log z$) fit to quasars (+) lying within the hemisphere centered on the CMBR dipole direction, while the dashed line is for the quasars (o) in the opposite hemisphere. From the CP, the two datasets otherwise are expected, statistically, to be similar in all respects. The finite displacement between the two straight line-fits, presumably therefore, is due to observer’s peculiar velocity, assumed to be a small non-relativistic value, with the displacement, to a first order, being proportional to the peculiar velocity component along the CMBR dipole.

to a first order, directly proportional to the amplitude of the peculiar velocity, assumed to be a small non-relativistic value. We can use a parameter p to express the peculiar velocity v , in units of the CMBR value, so that $v = p \times 370 \text{ km s}^{-1}$, with $p = 0$ implying a nil peculiar velocity while $p = 1$ implying the CMBR value. We show the loci of the expected displacements for different p from the continuous line ($p = 0$), by dotted lines for sources lying along the direction of the pole and by dashed lines for sources lying along the anti-pole direction. Figure 1 shows displacements expected for two values of the peculiar velocity ($p = 5$ and $p = 10$) by two dotted lines, which lie above the continuous line, i.e. at higher m_{w1} , and are representatives of the expected displacements for sources lying along the direction (pole) of the peculiar velocity at its apex. The dashed lines, on the other hand, drawn for two p values, $p = -5$ and $p = -10$, represent loci of the displacements expected for sources lying along the anti-pole direction ($p < 0$ in the anti-pole direction) and lie

below the continuous line, i.e. at lower m_{w1} . In Fig. 1, plots depicted for various p values are for sources exactly along the pole or anti-pole direction. For an even distribution of sources along various directions within each hemisphere, the net displacement will on average be half of that shown in Fig. 1 for each p value.

Figure 2 shows $m_{w1} - z$ plot for the quasars in our sample, separately for the two hemispheres, by a ‘+’ symbol for sources lying within the hemisphere Σ_1 , centered on the pole of the CMBR dipole, while ‘o’ symbol for sources lying in the opposite hemisphere Σ_2 , centered on the anti-pole. The dotted line shows the straight line ($m_{w1} \propto \log z$) fit to quasars lying within Σ_1 , while the dashed line is for the quasars lying within Σ_2 . From the CP, the two datasets statistically are expected otherwise to be similar in all respects. The finite displacement between the two straight line-fits, presumably therefore, is due to observer’s peculiar velocity, assumed to be a small non-relativistic value, with the displacement, to a first

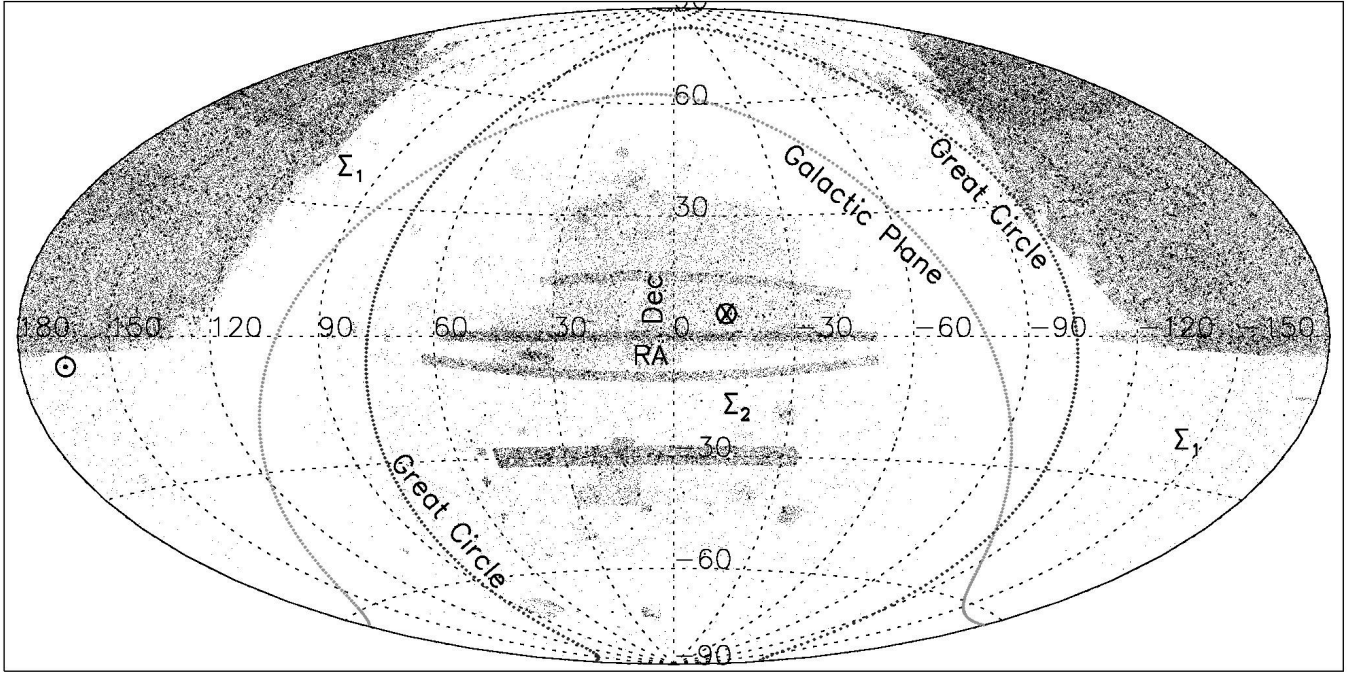


Figure 3. The sky distribution of $\sim 1.2 \times 10^5$ quasars in our sample, in the Hammer-Aitoff equal-area projection map, plotted in equatorial coordinates with right ascension (RA) from -180° to 180° and declination (Dec) from -90° to 90° . The distribution, as determined by the selection criteria for the spectroscopic redshift determination in various sub-samples, is not uniform across the sky. The sky position of the CMBR pole is indicated by \odot , while the corresponding anti-pole is indicated by \otimes . The great circle dividing the two hemispheres Σ_1 and Σ_2 is shown. Also shown is the galactic plane.

order, being proportional to the peculiar velocity component along the CMBR dipole.

If there were no peculiar motion (component) of the observer along that direction, then there should be no systematic shift in the magnitude-redshift diagram between the two datasets comprising sources belonging to the two opposite hemispheres. However due to a peculiar motion of the observer there will be alterations in the $m_{w1} - z$ plot, giving rise to the magnitude gap between the two fits. A comparison of the observed displacement between the dotted and dashed lines with those expected from fig. 1, assuming the quasars in our sample to be distributed uniformly over all polar angles with respect to the CMBR pole, suggests a large peculiar velocity $p \gtrsim 15$, instead of $p = 1$, expected from the CMBR dipole value. This inferred p value, at least to a first order, will be proportional to $\cos \psi$, the projection of the assumed dipole, CMBR here, on the direction of the actual dipole, if the two are different.

The sky distribution of quasars in our sample is displayed in fig. 3, where we have indicated the positions of the CMBR pole (\odot), and its anti-pole (\otimes). Also shown are the corresponding great circle dividing the two hemispheres Σ_1 and Σ_2 as well as the galactic plane. It is clear that the distribution of sources among Σ_1 and Σ_2 is not uniform by any standards. About 80% of the total quasars (89660 out of 115610) are in the hemispheres Σ_1 , almost all of these in the northern half of Σ_1 with only a small fraction in the southern part of Σ_1 . The remaining 20% (25950 quasars) lie in Σ_2 , with a rather patchy distribution (Fig. 3). What we really require in our method is that the sources in the sample at various redshifts

cover most polar angles reasonably well. Figure 4 shows the redshift (z) distribution against the polar angle θ , with respect to the CMBR pole, where quasars with $0^\circ \leq \theta \leq 90^\circ$ belong to the hemisphere Σ_1 while those with $90^\circ < \theta \leq 180^\circ$ belong to Σ_2 .

4 PROS AND CONS OF THE TECHNIQUE

The technique being applied here for estimating the peculiar motion of the observer from the Hubble diagram has certain advantages as compared to the elsewhere employed, alternate methods of deriving the peculiar motion from the dipole asymmetry in the number counts or sky brightness.

The other, alternate techniques, in order to determine the peculiar motion of the observer or equivalently of the Solar system with respect to the average universe, require samples comprising large numbers (millions!) of distant sources. This is because to measure equivalent of the CMBR dipole anisotropy $\sim 10^{-3}$, the number of sources required is of the order of $N \sim 10^6$ to achieve statistical uncertainty $\propto 1/\sqrt{N} \sim 10^{-3}$, to achieve a signal to noise of the order of unity (Crawford 2009; Singal 2011, 19a). Moreover, a uniform coverage of the whole sky (or at least a large fraction of it), with possibly only a small number of gaps, made from a single survey (to avoid different calibration scales in different surveys covering different parts of the sky which could in turn affect the number density of flux-limited samples in different directions differently, especially when the exercise depends upon the differential number density of sources observed in different directions to an accuracy of one part in

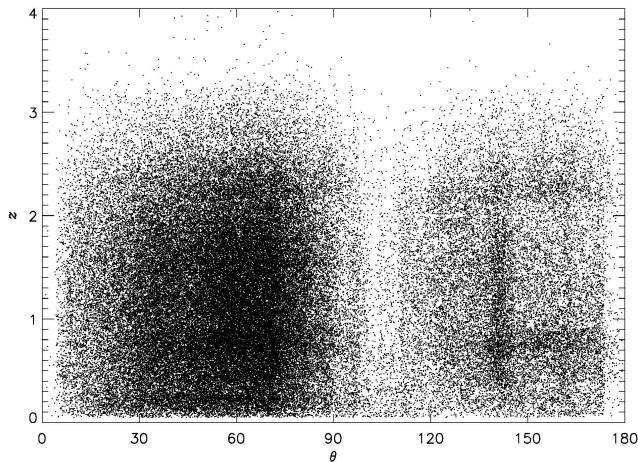


Figure 4. Redshift (z) distribution of quasars as a function of the polar angle θ with respect to the CMBR pole. Quasars with $0^\circ \leq \theta \leq 90^\circ$ belong to the hemisphere Σ_1 while those with $90^\circ < \theta \leq 180^\circ$ belong to Σ_2 .

10^3). Of course, a larger sample could help, however, a very careful matching of two or more surveys covering different parts of the sky with different flux-density limits that too at different frequencies of observations with different confusion limits is needed to get consistent results (Colin et al. 2017). Another complication that could arise from a use of two or more different survey data is apparent from the NVSS and TGSS surveys that yield dipole magnitudes which differ by more than a factor of two, so any overlaps of such samples could yield for the dipole magnitude very different values depending on how much is the overlap in the two such surveys and which survey is covering which particular regions of the sky.

However the present technique of employing the magnitude-redshift Hubble diagram to estimate the peculiar motion of the observer, does not depend upon a completeness of the survey, nor does it get much affected by a combination of data from a heterogeneous set of various sub-samples. Even a uniform coverage of the whole sky is not essential, all that one requires is that the properties of individual sources in the sample have not been systematically affected observationally, depending upon which region of the sky the source lies in. The conventional wisdom is that the reference frame of the CMBR, from the CP, is also a reference frame for the average distribution of *matter* in the Universe. However, in the last one decade it has been repeatedly seen (Singal 2011; Rubart & Schwarz 2013; Tiwari et al. 2015; Colin et al. 2017; Bengaly, Maartens & Santos 2018; Singal 2019a,b; Secrest et al. 2021; Singal 2021a,b,c) that the AGNS, which presumably are the best representatives of the average distribution of matter in the universe at large redshifts ($z \gtrsim 1$), do not seem to share the CMBR reference frame at much larger redshifts ($z \gtrsim 10^3$). Therefore it is necessary that we keep an open mind and try to determine the dipole that might represent the peculiar motion of the observer, moving as a part of the Solar system with respect to the average matter universe, by using as

many independent datasets, employing different methods, as possible.

In particular, the advantages of the present technique stem from (i) the Hubble diagram method for determining peculiar motion of the observer does not depend upon the exact nature of the $m - z$ relation or the underlying physics of the objects used in the sample. Nor does it depend upon the particular cosmological model to fit the $m - z$ relation. All is required is a phenomenological relation, that could be discerned in the $m - z$ plot. (ii) The completeness of the survey, where all sources above a flux density limit may be included in the basic surveys from which the sample may be derived, may not be a prerequisite here. (iii) The sample may not be having a uniform coverage of the sky; a piece-wise coverage of the sky in different directions could suffice, as long as the sources cover various different directions in the sky, so as to sample different projected components of the peculiar velocity. Therefore gaps in sky coverage or clustering of sources may not affect the results, as long as no other bias in $m - z$ plot, apart from the effects of the peculiar motion itself, gets introduced.

This technique has been successfully applied to determine the peculiar motion of the solar system, from the magnitude-redshift Hubble diagram for SNe Ia, which are one of the best standard candles known, with a very tight $m_B - z$ relation, where m_B denotes the observed peak in blue magnitude and z the measured redshift of each SN Ia. This technique could yield statistically significant results from a much smaller number of ($\lesssim 10^3$) SNe Ia (Singal 2021c).

In fact, this technique could as such be applied to a combination of data from a heterogeneous set of various sub-samples; all that is required is that no systematic errors have observationally entered in the redshift and magnitude estimates of individual sources depending upon the direction in sky. A very non-uniform sky coverage, as seen in Fig. 3, would have made it an almost meaningless exercise to try to get the peculiar motion from number counts or sky brightness, while from the Hubble diagram, as we shall show, we should be able to get values of the peculiar motion, even if with somewhat large errors.

On the negative side, the absence of a clear cut simple $m - z$ relation, for instance a straight line fit as seen in Fig. 1 could have made it difficult to figure out the differential effects of peculiar motion for sources in opposite hemisphere Σ_1 and Σ_2 . Or even a large spread in the magnitudes at any given redshift would increase the statistical uncertainties in the estimated peculiar velocity, both in its direction and amplitude.

5 DETERMINING THE DIRECTION AND AMPLITUDE OF THE PECULIAR MOTION

Since the direction of the quasar dipole might not be the same as that of any previously known dipole direction, including that of the CMBR, we want to determine the quasar dipole in a manner that is unbiased toward any particular direction. To achieve that, we employed the ‘brute force’ method (Singal 2019b), where we first divided the sky into $10^\circ \times 10^\circ$ pixels with minimal overlap, creating a grid of 422 cells covering the whole sky. Then taking the dipole direction to be centre of each of these 422 cells, in turn, we computed the dipole magnitude p (along with standard error) that provided the

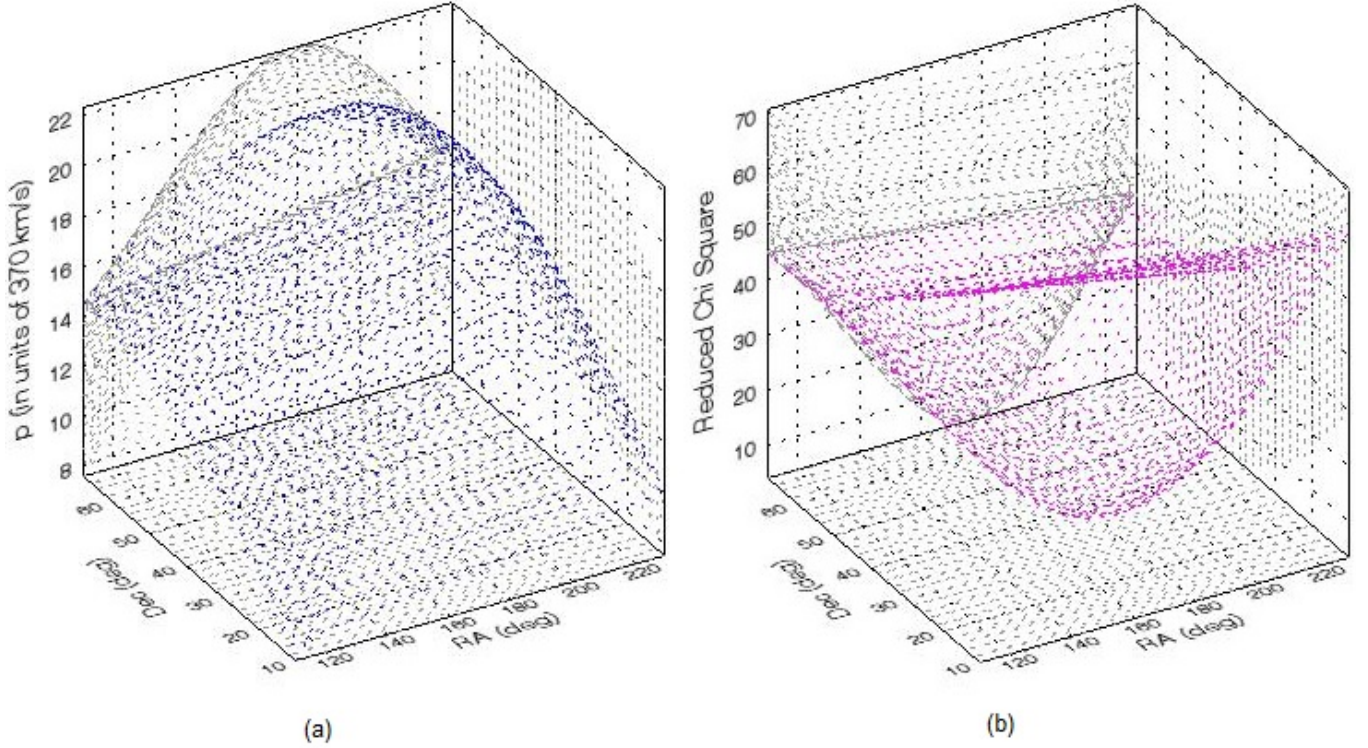


Figure 5. A 3-d plot (a) of the COSFIT routine result (in blue colour) for the trial dipole directions across the sky, showing a peak at RA= 180°, and Dec= 42° (b) of the reduced chi-square (χ^2_{ν}) values (in violet colour), from the cosfit routine for various trial directions for the dipole. The horizontal plane shows the direction in sky as RA and Dec in degrees. The minimum chi-square value of 3.7, somewhat higher than the ideal value of unity, occurs at RA= 177°, and Dec= 42°. The position of the extremum in each case is determined easily from the 2-d projections, shown in light grey. We infer the optimum direction of the observer's peculiar velocity to be RA= 179° ± 25°, and Dec= 42° ± 25°, which lies within 2σ of the CMBR Dipole direction, however has a rather large amplitude (higher by a factor of 22 ± 4).

best fit to the $m_{w1} - z$ data for the quasars in our sample. Actually this yields only a projection of the peculiar velocity in the direction of the pixel being tried. From all 422 p values, a broad plateau showing a maxima towards certain range of directions, not too far from the CMBR dipole direction, was though discernible, however, due to fluctuations in individual p values it was not possible to zero down on a single unique peak for the dipole direction. Since with respect to the actual dipole direction there should be a $\cos \theta$ dependence of the p values determined for other grid points, we made a 3-d $\cos \theta$ fit for each of the $n = 422$ positions for the remaining $n - 1$ p values, and also computed the chi-square value for each of these n fits.

The 3-d COSFIT resulted in a clear unique peak, with an accompanying minimum chi-square value in the near vicinity of the peak. The peak occurred at RA= 180°, Dec= 42°, with a height, $p = 22$. Figure 5 shows the 3-d COSFIT plot of the peak as well as a clear minimum in the reduced χ^2 value at RA= 178°, Dec= 42°. In order to make sure, we also tried finer grids with $5^\circ \times 5^\circ$ bins with 1668 cells and even a grid with $2^\circ \times 2^\circ$ bins with 10360 cells, but it made no perceptible difference in our results. Figure 5 shows the outputs of our COSFIT routine.

To test our COSFIT procedure, we made simulations, with random positions (RA and Dec) in sky allotted to quasars in

our sample and then a mock dipole in sky was superimposed to calculate z and m_{w1} for each source according to Eqs. (3) and (4). Then on this mock catalogue of quasars, our procedure was applied to recover the dipole and compared with the input dipole in that simulation. This not only validated our method but it also provided us an estimate of errors from 1500 independent simulations, in three sets of 500 each, so as to be sure that results from simulations, including error estimates, are consistent across different sets of simulations.

Accordingly, for the direction of the peculiar velocity we arrive at RA= 179°, Dec= 42° from the minimum value of the Chi-square fit as well as from the peak in dipole magnitude, with both almost coinciding. Estimated errors in the dipole are $\Delta \text{RA} = \pm 25^\circ$ and $\Delta \text{Dec} = \pm 25^\circ$. This value for the derived quasar dipole direction agrees, within the 2σ uncertainty, with the CMBR dipole direction, RA= 168°, Dec= -7°. However the magnitude of the quasar dipole corresponds to with $p = 22 \pm 4$, or a solar speed $8.1 \pm 1.5 \times 10^3 \text{ km s}^{-1}$, a 5.4σ result.

Figure 6 shows, for observer's peculiar velocity direction along RA=179°, Dec=42°, the expected differences in magnitude, Δm_{w1} , as a function of redshift (z), between sources from the two hemispheres, Σ_1 and Σ_2 , plotted as dotted lines, for different peculiar velocity values ($p = 0$ to 35). The unbroken line shows a fit to the actual observed difference between

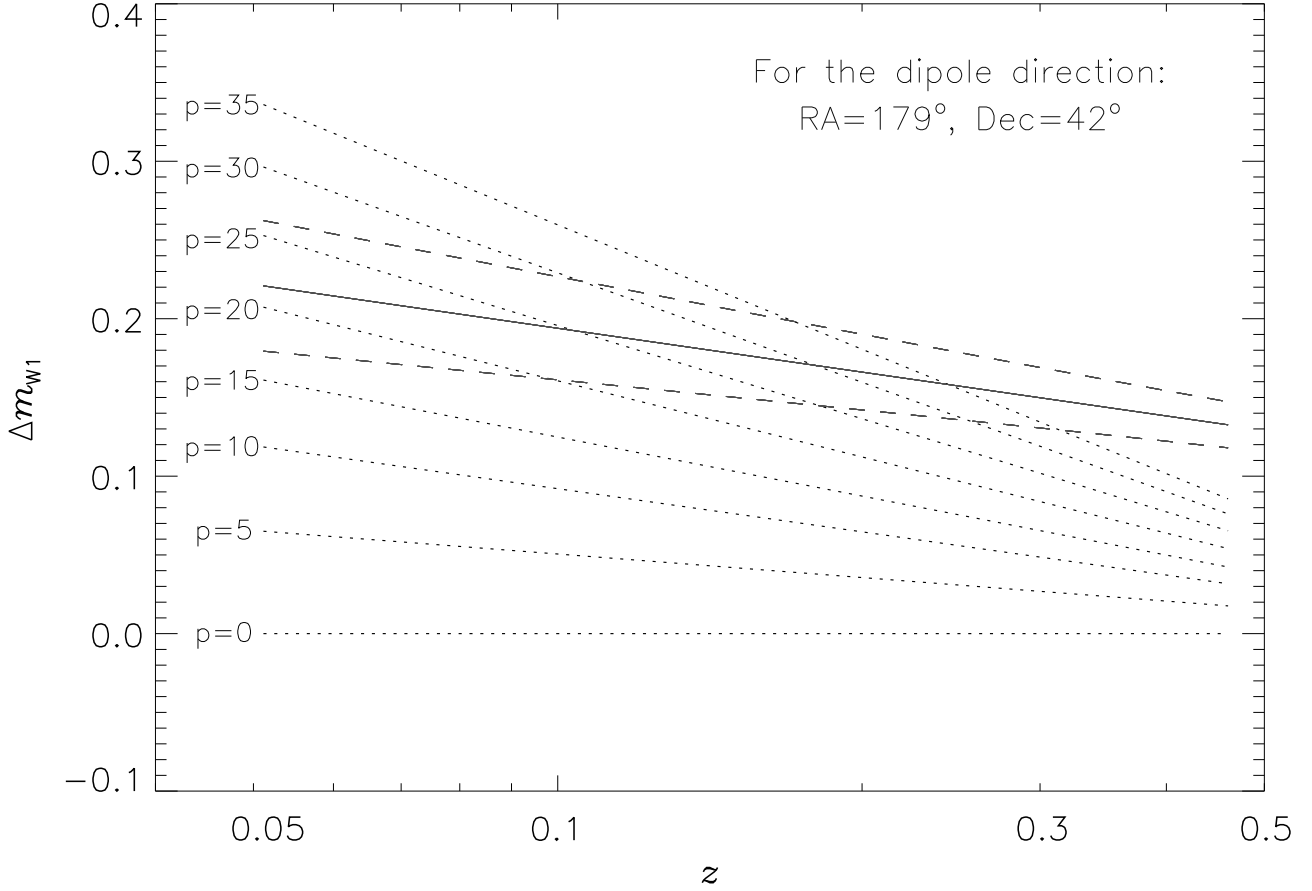


Figure 6. For observer’s peculiar velocity direction along $RA=179^\circ$, $Dec=42^\circ$, the expected differences in magnitude, Δm_{w1} , as a function of redshift (z), between sources from the two hemispheres, Σ_1 and Σ_2 , plotted as dotted lines, for different peculiar velocity values ($p = 0$ to 35). The unbroken line shows a fit to the actual observed difference between the average magnitudes of sources from the two hemispheres, at different redshifts, while the dashed lines above and below the unbroken line represent the 1σ uncertainties in the fit.

the average magnitudes of sources from the two hemispheres, at different redshifts, while the dashed lines above and below the unbroken line represent the 1σ uncertainties in the fit. We get $p = 22 \pm 4$ for the peculiar velocity.

Since the method does not depend upon the number of sources in the sample, apart from that the errors may increase for a smaller number of sources, we split our sample into two, by picking the odd and even serial number sources in the original sample and separately combining them to get two sub-samples and then following our above procedure, determined the peculiar motion from the two sub-samples independently. The results that we thus got for the dipole values were $p = 22 \pm 6.5$ along $RA = 185^\circ$, $Dec = 46^\circ$ and $p = 22 \pm 6$ along $RA = 172^\circ$, $Dec = 38^\circ$. These are consistent with the value, $p = 22 \pm 4$ along $RA = 179^\circ$, $Dec = 42^\circ$ derived from the whole sample, with no unexpected variations in the results from the two sub-samples. This supports the view that the shift in the Hubble diagram between the two set of sources belonging to opposite hemispheres is a genuine effect, presumed to be a result of the observer’s peculiar motion, and not arising from

some skew distribution among some small number of sources in either dataset.

6 IMPLICATIONS FOR THE COSMOLOGICAL PRINCIPLE

In order to compare our results with earlier dipoles determined from different datasets, we show in Fig. 7 the relative positions of the estimated directions of various dipoles in a relevant portion of the sky. The position of the pole determined from the Hubble diagram of our quasar sample, indicated by H , is shown along with the error ellipse. Also shown are the pole positions for other dipoles, along with their error ellipses: N (NVSS) (Singal 2011), T (TGSS) (Singal 2019a), Z (DR12Q) (Singal 2019b), M (MIRAGN) (Singal 2021a,b), S (SNe Ia) (Singal 2021c). The CMBR pole, at $RA = 168^\circ$, $Dec = -7^\circ$, indicated by \odot , has negligible errors (Aghanim et al. 2020). It seems that the poles of the dipole from the Hubble diagram as well as of mid-infrared quasars lie within 2σ of the CMBR pole, but each of the other four dipoles lies

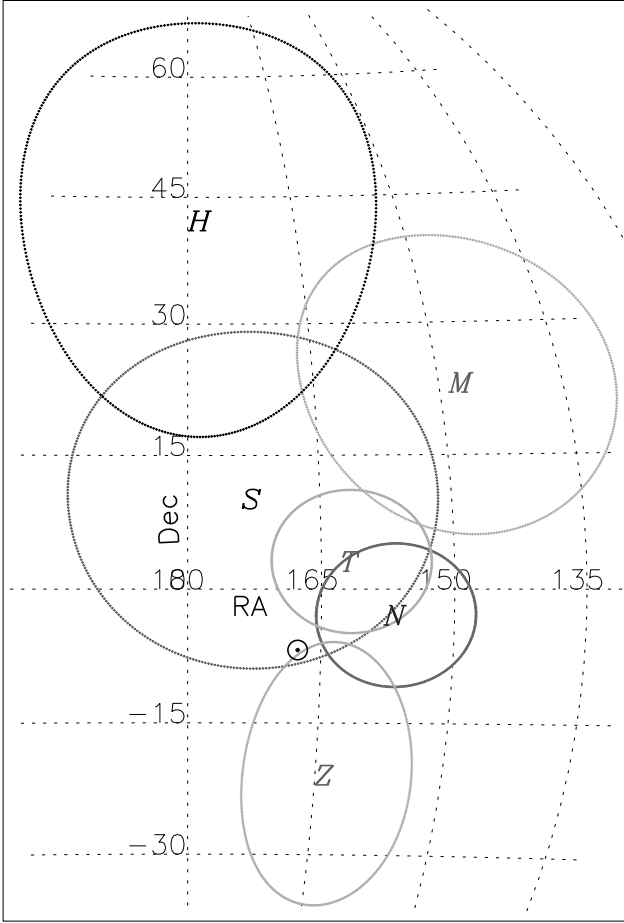


Figure 7. A small portion of the sky, in the Hammer–Aitoff equal-area projection, plotted in equatorial coordinates RA and Dec, showing the position of the pole determined from the Hubble diagram of our quasar sample, indicated by *H*, along with the error ellipse. Also shown on the map are the other pole positions for various dipoles along with their error ellipses, *N* (NVSS), *T* (TGSS), *Z* (DR12Q), *M* (MIRAGN), *S* (SNe Ia). The CMBR pole, at RA= 168°, Dec= −7°, indicated by \odot , has negligible errors.

within $\sim 1\sigma$ of the CMBR pole. From that we can surmise that the various dipoles, including the CMBR dipole, are all pointing along the same direction. Nevertheless, it is evident that all these other dipoles have much larger amplitudes than the CMBR dipole, with almost an order of magnitude spread, even though various dipole directions in the sky may be lying parallel to each other. From various dipoles we cannot arrive at a single coherent picture of the solar peculiar velocity, which, defined as a motion relative to the local comoving coordinates and from the CP, a motion with respect to an average universe, should after all not depend upon the exact method used for its determination.

There are other alternative models put forward for the dipoles, e.g., the Hubble parameter being higher in the direction of the CMBR dipole at higher redshifts ($z \sim 1$) has been suggested (Krishnan 2021a,b). Also there is a model suggested for a “dark flow” dipole at the position of galaxy clusters, found in filtered maps of the CMBR temperature anisotropies, implying the existence of a primordial CMBR

dipole of non-kinematic origin (Kashlinsky 2008,09,10; Atrio-Barandela 2015). Based on study of quasar absorption systems, a dipole in the spatial variation of the fine-structure constant, $\alpha = e^2/\hbar c$ has also been reported (Webb et al. 2011; King et al. 2012; Berengut et al. 2011; Berengut, Kava, & Flambaum 2012) and these spatial variations of α could be constrained using clusters of galaxies (Galli 2013; Martino et al. 2016). It has been claimed that the fine structure constant cosmic dipole is aligned with the corresponding dark energy dipole within 1σ uncertainties (Mariano & Perivolaropoulos 2012,13). Further, the odd multipoles in the large scale anisotropies of the CMB temperature, a parity asymmetry, show a preference to be strongly aligned with the CMBR dipole at significant levels (Naselsky et al. 2012; Zhao 2014; Cheng et al. 2016). All such alignments are inconsistent with the CP and the ensuing standard model.

The observed fact that different dipoles, resulting from different, independent datasets, obtained with independent instruments and techniques in different wavebands by different independent groups, happen to be pointing along the same direction in sky, shows that these dipoles are not results of some systematics in individual datasets, otherwise they would have been pointing in random directions in sky. This particular direction in sky must have some peculiarity and is in some respects a preferred direction, a sort of an “axis” of the universe. In any case, so many independent dipole vectors pointing along the same particular direction could imply an anisotropic universe, violating the CP, a cornerstone of the modern cosmology.

7 CONCLUSIONS

From the Hubble diagram of quasars, peculiar motion of the Solar system is derived, which turns out to be the largest value ever found and is more than about 20 times larger than that inferred from the CMBR dipole, though the direction lies within 2σ of the CMBR dipole. It seems that the dipoles determined from the AGNs, or even from SNe Ia, somehow have much larger amplitudes than the CMBR dipole, with almost an order of magnitude spread, coinciding neither with each other nor with the CMBR, though their directions coincide within statistical uncertainties. It shows that they are not randomly oriented and that the various dipoles, including the CMBR dipole, are all pointing along the same direction, suggesting a preferred direction in the Universe, thereby raising uncomfortable questions about the CP, the basis of the standard model in modern cosmology.

DATA AVAILABILITY

The data underlying this article is freely available at VizieR Astronomical Server in the public domain (<http://vizier.u-strasbg.fr/viz-bin/VizieR>) and can be downloaded by selecting the catalog: J/ApJS/221/12/table1.

REFERENCES

- Aghanim N., Akrami T., Arroja F. et al., 2020, *A&A*, 641, A1
 Atrio-Barandela, F., Kashlinsky, A., Ebeling, H., Fixsen, D. J., Kocevski, D. 2015, *ApJ*, 810, 143

- Bengaly C. A. P., Maartens R., Santos M. G., 2018, *J. Cosm. Astropart. Phys.*, 4, 31
- Berengut, J. C., Flambaum, V. V., King, J. A., Curran, S. J., Webb, J. K., 2011, *Phys. Rev. D*, 83, 123506
- Berengut, J. C., Kava, E. M., Flambaum, V. V., 2012, *ibid.*, 85, 054011
- Cheng, C., Zhao, W., Huang, Q.-G., Santos, L., 2016, *Phys. Lett. B*, 757, 445
- Colin J., Mohayaee R., Rameez M., Sarkar S., 2017, *MNRAS*, 471, 1045
- Crawford F., 2009, *ApJ*, 692, 887
- Davis T. M., Hui L., Frieman J. A. et al., 2011, *ApJ*, 741, 67
- Galli, S., 2013, *Phys. Rev. D*, 87, 123516
- Hinshaw G., Weiland J. L., Hill R. S. et al., 2009, *ApJS*, 180, 225
- Kashlinsky, A., Atrio-Barandela, F., Kocevski, D., Ebeling, H., 2008, *ApJ*, 686, 498
- Kashlinsky, A., Atrio-Barandela, F., Kocevski, D., Ebeling, H., 2009, *ApJ*, 691, 1479
- Kashlinsky, A., Atrio-Barandela, F., Ebeling, H., Edge, A., Kocevski, D., 2010, *ApJ*, 712, L81
- King, J. A., Webb, J. K., Murphy, M. T., Flambaum, V. V., Carswell, R. F., Bainbridge, M. B., Wilczynska, M. R., Koch, F. E., 2012, *MNRAS*, 422, 3370
- Krishnan, C., Mohayaee, R., Ó Colgáin, E., Sheikh-Jabbari, M. M., Yin, L., 2021, *arXiv:2105.09790*
- Krishnan, C., Mohayaee, R., Ó Colgáin, E., Sheikh-Jabbari, M. M., Yin, L., 2021, *arXiv:2106.02532*
- Lineweaver C. H., Tenorio L., Smoot G. F., Keegstra P., Banday A. J., Lubin P., 1996, *ApJ*, 470, 38
- Mainzer, A., Bauer, J., Cutri, R. M. et al., 2014, *ApJ*, 792, 30
- Mariano, A., Perivolaropoulos, L., 2012, *Phys. Rev. D*, 86, 083517
- Mariano, A., Perivolaropoulos, L., 2013, *Phys. Rev. D*, 87, 043511
- Martino, I. De, Martins, C. J. A. P., Ebeling, H., Kocevski, D., 2016, *Phys. Rev. D*, 94, 083008
- Naselsky, P., Zhao, W., Kim, J., Chen, S., 2012, *ApJ*, 749, 31
- Rubart M., Schwarz D. J., 2013, *A&A*, 555, A117
- Secrest N. J., Dudik R. P., Dorland B. N., Zacharias N., Makarov V., Fey A., Frouard J., Finch, C., 2015, *ApJS*, 221, 12
- Secrest N. J., Hausegger S. V., Rameez M., Mohayaee R., Sarkar S., Colin J., 2021, *ApJ*, 908, L51
- Singal A. K., 2011, *ApJ*, 742, L23
- Singal A. K., 2019a, *Phys. Rev. D*, 100, 063501
- Singal A. K., 2019b, *MNRAS*, 488, L104
- Singal, A. K., 2021a, *SPProc. 1st Electronic Conference on Universe 2021 (ECU2021)*, doi:10.3390/ECU2021-09270
- Singal A. K., 2021b, *Universe* 7, 107
- Singal A. K., 2021c, *arXiv:2106.11968*
- Tiwari P., Kothari R., Naskar A., Nadkarni-Ghosh S., Jain P., 2015, *Astropart. Phys.*, 61, 1
- Webb, J. K., King, J. A., Murphy, M. T., Flambaum, V. V., Carswell, R. F., Bainbridge, M. B., 2011, *Phys. Rev. Lett.*, 107, 191101
- Wright, E. L., Eisenhardt, P. R. M., Mainzer, A. K. et al., 2010 *AJ*, 140, 1868
- Zhao, W., 2014, *Phys. Rev. D*, 89, 023010